Erosive Burning of Composite Solid Propellants: Mechanism, Correlation, and Grain Design Applications

R. Arora,* X. Wu,† F.X. White,‡ and K.K. Kuo§
The Pennsylvania State University, University Park, Pennsylvania

With increasing interest evidenced in the development of nozzleless and high-performance solid rocket motors, an understanding of the erosive-burning characteristics of solid propellants in high-velocity cross flows is important in establishment of grain design procedures. A theoretical model based on a turbulent reacting boundary-layer analysis, validated with experimental data, was used to conduct parametric studies under broad ranges of Mach number, pressure, surface roughness, pressure gradient, port diameter, and propellant initial temperature. Using nonlinear regression analysis, an erosive-burning rate correlation was developed in terms of the cited parameters. The results for two motor grain contours were used to demonstrate the applicability of this correlation to grain design.

Nomenclature

a = pre-exponent in strand burning rate law, cm/s/(MPa)^n
A_s = Arrhenius frequency factor in surface decomposition, m/s
C_s = heat capacity of solid propellant, kcal/kg-K
C_p = average heat capacity of reacting gases, kcal/kg-K, $\equiv \sum_k Y_k C_{p_k}$
D = port diameter, m
E_{as} = activation energy in solid-surface decomposition, kcal/mole
f_D = burning rate correction factor for effect of port diameter
$f_{M,P}$ = burning rate correction factor for effect of Mach number and pressure
f_{PG} = burning rate correction factor for effect of pressure gradient
f_{Rh} = burning rate correction factor for effect of roughness
$\Delta h^0_{f,k}$ = heat of formation of kth species, kcal/kg
M = Mach number
n = exponent in the strand burning-rate law
P = pressure, MPa
$\bar{Q}_s$ = net surface heat release (negative for exothermic reactions), kcal/kg
r_b = propellant burning rate, cm/s
R_h = roughness height, μm
Tpi = initial propellant temperature, K
$\bar{T}ps$ = reference surface temperature used to measure $\bar{Q}_s$, K
W_k = molecular weight of kth species, kg/kmole
Y_{FS} = mass fraction of fuel in propellant
Y_{OS} = mass fraction of oxidizer in propellant
γ = ratio of constant-pressure and constant-volume specific heats
ν_k = mole fraction of kth species
ρ_s = solid propellant density, kg/m^3
σ_p = temperature sensitivity, K^{-1}

Superscript

o = strand burning conditions

Subscripts

D = port diameter
PG = pressure gradient
r = reference
R = rough surface
S = smooth surface
th = threshold

Presented as Paper 81-1581 at the AIAA/SAE/ASME 17th Joint Propulsion Conference, Colorado Springs, Colo., July 27-29, 1981; submitted Sept. 23, 1981; revision received May 24, 1982.

*Research Assistant, Mechanical Engineering Department.Student Member AIAA.
†Adjunt Research Associate, Mechanical Engineering Department.
‡Undergraduate Assistant, Mechanical Engineering Department.
§Professor, Mechanical Engineering Department. Associate Fellow AIAA.

Introduction

THE burning rate of solid propellants has been found to be augmented by the flow of product gases across the burning surface. This phenomenon, known as erosive burning, occurs commonly in solid propellant rocket motors, and particularly in nozzleless motors, or those with small port-to-throat area ratios. In these motors, the erosive-burning augmentation can be extremely high, leading to high-pressure transients and consequent unequal propellant burning rates. Chamber conditions also vary along the axial direction, leading to uneven burning rates.

Optimal design of a rocket motor grain requires accurate prediction of the propellant burning rate under a range of important parameters. This predictive ability enables motor designers to specify a combination of propellant formulations and grain geometry to achieve such desired rocket motor characteristics as thrust level, burning time, and minimum propellant residual. In the past, various methods were used to investigate erosive burning; details can be found in recent literature reviews by Kuo and Razdan[1] and King.[2] Results of some recent studies are summarized in a report by King et al.[3]

In general, one of three approaches can be used to estimate the erosive-burning rate of a solid propellant: 1) interpolation from existing tabulated erosive-burning experimental data, 2) numerical solution of the reacting turbulent boundary-layer equations, or 3) use of empirical or phenomenological erosive-burning correlations.

The first approach is obviously very limited since experimental data for a wide range of all important parameters

is required for each propellant considered. The second approach is the most complete of the three for the region where such an analysis is valid, but can be prohibitively expensive in terms of computer costs. The third approach has the advantage of simplicity of application as well as a wide range of applicability, provided the particular correlation considered involves all relevant parameters. Most of the correlations developed to predict the erosive-burning rate depend only on parameters such as velocity (or Mach number), pressure, strand-burning rate, and/or mass flow rate. However, both theoretical and experimental studies demonstrate that the actual burning rate also depends on other factors, including propellant surface roughness height, flow pressure gradient, port radius, and initial propellant temperature, and that the influence of these factors is not always negligible. Therefore, a correlation is needed which includes the appropriate effect of all of the parameters; this is the prime motivation of the present paper.

A model[4-6] utilizing the second approach to predict erosive-burning rates of composite solid propellants has been developed at The Pennsylvania State University. The code utilizes Patankar and Spalding's[7] method to solve the partial-differential equations describing reacting turbulent boundary-layer flows. Since the code is based on the boundary-layer assumptions, it should be used only for regions where a shear layer exists over the surface. Therefore, the model is not applicable to regions with very high values of blowing parameter or very low values of cross-flow velocity, where the boundary layer may not exist. This is not viewed by the authors as a serious limitation, since most rocket motors do have a shear layer over part of the propellant surface. Comparisons of predictions of this program with the experimental data of Marklund and Lake[8] and Razdan and Kuo[9] show good agreement.[9,10] Since this model has been proven successful in predicting erosive-burning rates of several composite solid propellants under various flow conditions, and is considered a reliable means of generating "data," parametric runs with this code were made to obtain data which could then be used to develop correlations relating all parameters considered. Algebraic expressions obtained in this manner can readily be used for grain design. This procedure enables grain designers to bypass the expensive and time-consuming repetitive solution of partial-differential equations, and still obtain results of good accuracy.

Two rocket motor grain contours were analyzed, using this code, to show the characteristic variation of flow properties with radial and axial location. Profiles obtained are used to illustrate the physical mechanism of erosive burning at various locations in the motor.

The specific propellant used in this study was a typical AP-based composite solid propellant. However, the overall approach and conclusions should be applicable to most AP-based composite solid propellants. The functional form of the correlation was developed by examining the trends in the parametric data. This form can also be used as a guideline for obtaining empirical constants required for similar correlations applicable to other propellants.

Method of Approach

Background

The erosive burning code (EBC) was developed at The Pennsylvania State University to predict burning rates of composite solid propellants under strong cross-flow conditions. The physical model considered in the theoretical analysis consists of flow of gases 1) over a flat plate, or 2) inside a duct. Following the procedure detailed in Ref. 5, the general conservation equations for turbulent-reacting compressible fluid flow are reduced to a system of seven coupled, inhomogeneous, partial-differential equations. These are the conservation equations of mass, momentum, fuel and oxidizer species, enthalpy, turbulence kinetic energy, and turbulence dissipation. Spalding's eddy-break-up model[11] is used to evaluate the rate of consumption of reactant species. Turbulence closure models used, modeling of the gas-phase chemical reactions, boundary conditions applied, and the near-wall treatment required for the k-ϵ closure are all detailed in Ref. 10. These equations are then solved numerically by applying the transformations and finite difference procedure suggested by Patankar and Spalding.[7] The code has been tested against a wide range of experimental data; the results of these comparisons are described in Ref. 10.

For the present study, the propellant selected was an AP/PBAA-EPON formulation with well-documented physicochemical properties and strand-burning characteristics. Input data for this propellant are listed in Table 1. It may be noted that the value of $\overline{Q}_s$ used in this study was determined by matching the predicted results for one set of experimental conditions. This value was then tested for a wide range of conditions and was found to give good agreement between experimental and theoretical results. The same value of $\overline{Q}_s$ was also used to obtain the results described in Refs. 3, 5, 6, 9, and 10.

After several preliminary runs of EBC, the following parameters were identified as potentially significant: Mach number (M), pressure (P), propellant surface roughness height (R_h), initial propellant temperature (Tpi), pressure gradient ($\partial P/\partial x$), and port diameter (D). A set of typical values for these parameters was chosen as the baseline case. These are given in Table 2. The parameters were then selectively perturbed from the baseline case to determine their independent or joint influence on the erosive-burning rate augmentation factor, r_b/r_b^0. The range of variation of the selected parameters is also given in Table 2. Using data obtained in this way, the functional forms of the tentative correlations could be conjectured and refined by means of nonlinear regression analysis. The details of this procedure and the final correlations are presented in the following section.

Table 1 Properties of AP/PBAA-EPON (75/25) propellant[6]

$a = 0.2452$ cm/s/(MPa)^n	$\bar{T}ps = 800.0$ K
$A_s = 5.65$ m/s	$W_F = 30.000$ kg/kmole
$C_s = 0.3$ kcal/kg-K	$W_0 = 27.893$ kg/kmole
$C_p = 0.3$ kcal/kg-K	$W_p = 20.381$ kg/kmole
$E_{as} = 15.0$ kcal/mole	$Y_{FS} = 0.25$
$\Delta h^0_{f,F} = 55.93$ kcal/kg	$Y_{OS} = 0.75$
$\Delta h^0_{f,0} = -942.0$ kcal/kg	$\gamma = 1.26$
$\Delta h^0_{f,P} = -1137.3$ kcal/kg	$\nu_F = 1.00$ mole
$n = 0.41$	$\nu_0 = 3.2266$ mole
$\overline{Q}_s = -250.0$ kcal/kg	$\nu_P = 5.888$ mole
$\sigma_p^0 = 0.002$ K^{-1}	$\rho_s = 1600.0$ kg/m^3

Table 2 Baseline case parameters

Parameters	Baseline values	Range of values
$M(-)$	0.5 for $M<1$	0.25→1.0
	1.5 for $M>1$	1.0→2.4
P, MPa	5.0	2.5→7.7
R_h, μm	0	0→40
Tpi, K	298	215→330
$\partial P/\partial x$, MPa/m	0	−10.0→0
D,m	∞	0.02→∞

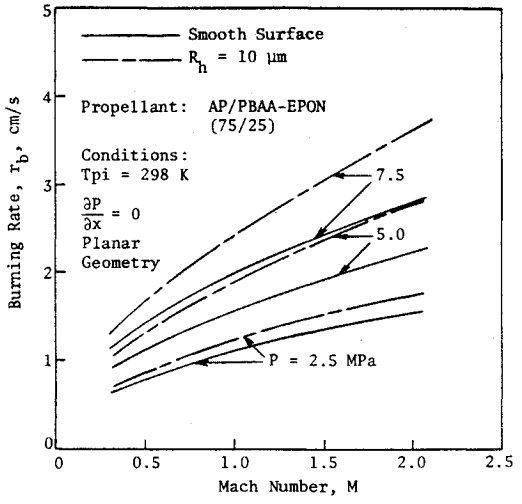

Fig. 1 Effects of Mach number, pressure, and surface roughness on burning rate.

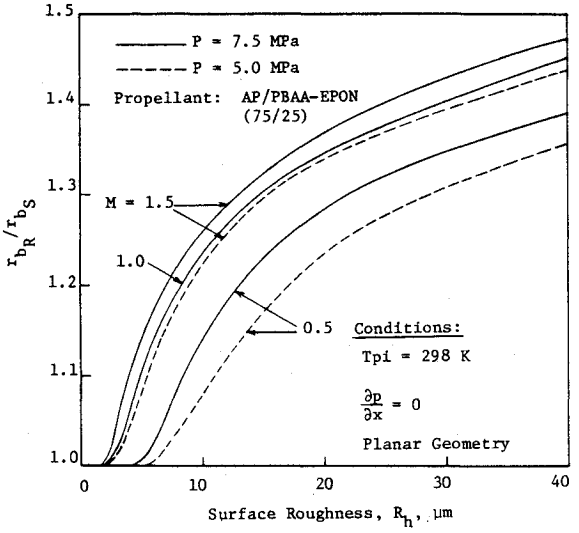

Fig. 2 Effect of surface roughness on burning rate.

Development of Correlations

The first set of data represents the variation of r_{b_S} (burning rate of propellant with hydrodynamically smooth surface) vs cross-flow Mach number for different values of pressure, and are plotted as solid lines in Fig. 1. The trends of the data indicate that an expression of the form

$$r_{b_{S,Tpi_r,0,\infty}} - r^0_{b_{Tpi_r}} = C_1 M^{C_2} P^{C_3} \tag{1}$$

is a fair representation of the results. In Eq. (1), the four subscripts of r_b denote smooth surface (S), reference initial propellant temperature (Tpi_r), zero pressure gradient (PG = 0), and planar geometry ($D = \infty$), respectively. Preliminary regression analysis suggested that $(M - M_{th})P$ may correlate well as a group, where M_{th} represents a threshold Mach number. This was borne out by subsequent analysis, and the final form of the M,P correction factor was

$$f_{M,P} \equiv \frac{r_{b_{S,Tpi_r,0,\infty}} - r^0_{b_{Tpi_r}}}{r^0_{b_{Tpi_r}}}$$

$$= \frac{0.40[(M - M_{th})P]^{0.64}}{aP^n} \quad \text{if} \quad M > M_{th}$$

$$= 0 \quad \text{if} \quad M \le M_{th} \tag{2}$$

For the propellant considered, the value of M_{th} was found to be zero. Tpi_r was set to equal to 298 K.

It may be noted that M in this expression is M_e, the Mach number at the edge of the boundary layer, as distinct from $\overline{M}$, the one-dimensional Mach number. Either of these two Mach numbers can be selected for the correlation, but M_e was chosen for the following reasons. 1) Erosive burning is a phenomenon caused by the shear action in the boundary layer. (Physically, therefore, M_e is a more meaningful parameter.) 2) Two channel flows can have an identical $\overline{M}$, but different M_e's corresponding to different boundary-layer profiles. The boundary-layer characteristics, therefore, cannot be represented by $\overline{M}$.

Figure 1 also indicates the influence of surface roughness on the burning rate, as shown by the dashed lines; r_b increases with roughness height. This effect was investigated in detail and the results are plotted in Fig. 2. As can be seen from Fig. 2, the degree of influence of R_h on r_{b_R}/r_{b_S} is dependent on the Mach number and pressure. It was also noted that the curves of r_{b_R}/r_{b_S} vs R_h for the same value of the product of M and P were very close. This implies that the correlation should involve MP as a single parameter. The actual shapes of the curves suggested that a tanh function may well represent all the data presented in Fig. 2. Based on these observations, the correction factor developed for propellants with rough burning surface, is

$$f_{R_h} \equiv \frac{r_{b_{R,Tpi_r,0,\infty}} - r^0_{b_{Tpi_r}}}{r_{b_{S,Tpi_r,0,\infty}} - r^0_{b_{Tpi_r}}}$$

$$= 1 + 0.50 \tanh[0.063(MP)^{0.59}R_h - 1]$$

$$= 1 \quad \text{if} \quad [0.063(MP)^{0.59}R_h - 1] < 0 \tag{3}$$

This expression also serves to define a threshold roughness, below which the influence of roughness is effectively zero. The threshold roughness defined in this manner is

$$R_{h_{th}} = [0.063(MP)^{0.59}]^{-1} \tag{4}$$

It has a realistic dependence on M and P (see Fig. 2), since the value of $R_{h_{th}}$ decreases as MP increases.

It is a well-known fact that pressure gradients exist in the port of a motor grain, especially for high-loading density grains. The influence of pressure gradient on the erosive-burning rate was investigated by using data with constant values of R_h and MP to isolate the effect of $\partial P/\partial x$. A set of typical results, for $MP = 4.73$ and $R = 0$, is shown in Fig. 3. The linear variation of the ordinate with $\partial P/\partial x$ was noted from the data, and was confirmed by a preliminary nonlinear regression analysis which yielded an exponent of $\partial P/\partial x$ close to 1.0. Very similar results were also obtained for other values of MP and R_h, indicating that the pressure gradient influence is not a function of R_h, M, or P. The resulting correction factor is

$$f_{PG} \equiv \frac{r_{b_{R,Tpi_r PG,\infty}} - r^0_{b_{Tpi_r}}}{r_{b_{R,Tpi_r,0,\infty}}} = 1 - 0.019\frac{\partial P}{\partial x} \tag{5}$$

Comparison of predicted erosive-burning rates for two-dimensional and axisymmetric cases showed that the port diameter (D) does have a certain influence, particularly for small values of D. This effect has also been noted by Yezzi et al.[12] It is desirable, then, to be able to predict the effect of curvature on the erosive-burning rate. Parametric runs for various radii were conducted, but it was difficult to totally isolate the curvature effect from that of the other parameters, e.g., pressure gradient. Figure 4 shows the effect of port diameter on burning rate. The scatter of numerical data on

this figure is due to variation of other flow parameters. However, the degree of scatter is still small enough to allow development of a correction term for this effect. In order to attain the asymptotic limit of planar geometry, an exponential function was selected. The curvature correction factor developed can be expressed as

$$f_D = 1 + 0.1\exp(-2.8D) \tag{6}$$

where

$$f_D \equiv \frac{r_{b_{R,Tpi_r,\mathrm{PG},D}} - r^0_{b_{Tpi_r}}}{r_{b_{R,Tpi_r,\mathrm{PG},\infty}} - r^0_{b_{Tpi_r}}}$$

The next parameter considered was the initial propellant temperature, *Tpi*. The temperature sensitivity of strand-burning rate, σ_p^0, is conventionally defined as

$$\sigma_p^0 \equiv \left[\frac{\partial(\ell n r_b^0)}{\partial Tpi}\right]_P \tag{7}$$

To clarify the influence of initial propellant temperature on erosive-burning rate, let us define

$$\sigma_p \equiv \left[\frac{\partial(\ell n r_b)}{\partial Tpi}\right]_P \tag{8}$$

If we plot the logarithmic variation of the burning-rate ratio vs $(Tpi - Tpi_r)$, as in Fig. 5, it is apparent that for the *Tpi* range considered, the ordinate has a nearly linear variation with $(Tpi - Tpi_r)$. The influence of *M* and *P* on the ordinate is seen to be negligible. These observations imply that σ_p as defined in Eq. (8) is a useful parameter, and that it is essentially independent of *M* and *P*. Another important observation can be made by comparing the values of σ_p^0 and σ_p which are 0.20×10^{-2} K^{-1} and 0.16×10^{-2} K^{-1}, respectively. This comparison shows that the presence of a cross flow decreases the sensitivity of r_b to *Tpi*. The correction factor is given by

$$\frac{r_{b_{R,Tpi,\mathrm{PG},D}}}{r^0_{b_{Tpi}}} = \frac{r_{b_{R,Tpi_r,\mathrm{PG},D}}}{r^0_{b_{Tpi_r}}} \frac{\exp[\sigma_p(Tpi - Tpi_r)]}{\exp[\sigma_p^0(Tpi - Tpi_r)]} \tag{9}$$

To develop an overall erosive-burning rate correlation, the preceding correction factors can be combined as follows. By multiplying the burning rate ratios of Eqs. (2), (3), (5), and (6), we obtain

$$\frac{r_{b_{R,Tpi_r,\mathrm{PG},D}}}{r^0_{b_{Tpi_r}}} - 1 = f_{M,P} f_{R_h} f_{\mathrm{PG}} f_D \tag{10}$$

Then, substituting Eq. (10) into Eq. (9), the overall erosive-burning rate predictive correlation becomes

$$\frac{r_{b_{R,Tpi,\mathrm{PG},D}}}{r^0_{b_{Tpi}}} = (1 + f_{M,P} f_{R_h} f_{\mathrm{PG}} f_D)\exp[(\sigma_p - \sigma_p^0)(Tpi - Tpi_r)] \tag{11}$$

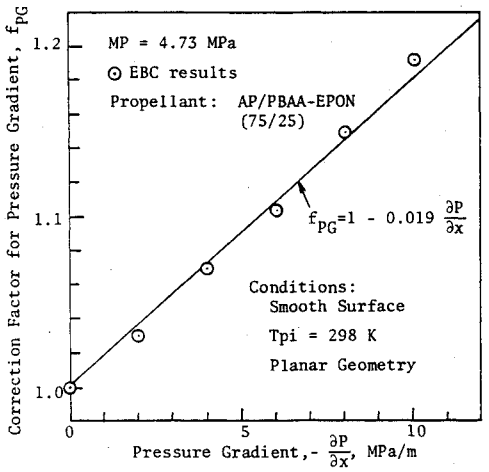

Fig. 3 Correction factor f_{PG} as a function of pressure gradient.

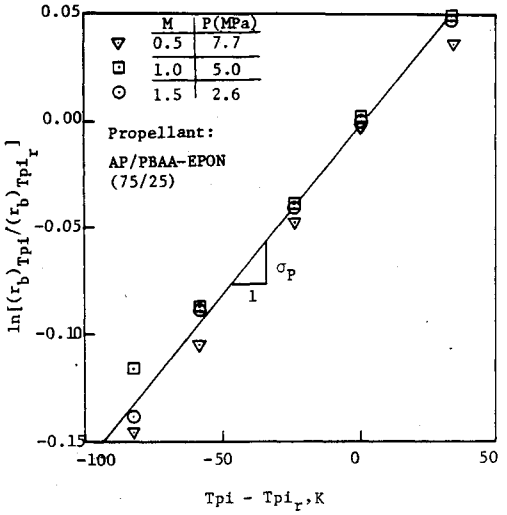

Fig. 5 Effect of propellant initial temperature on burning rate.

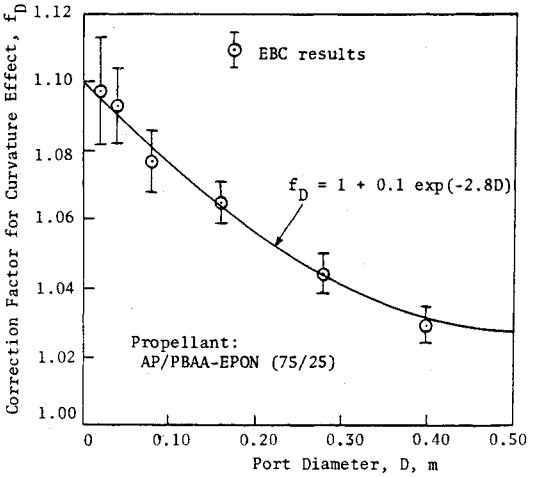

Fig. 4 Correction factor f_D as a function of port diameter.

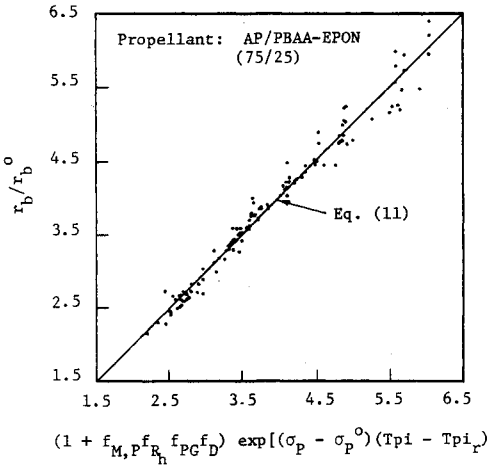

Fig. 6 Comparison of erosive burning data from EBC with overall correlation.

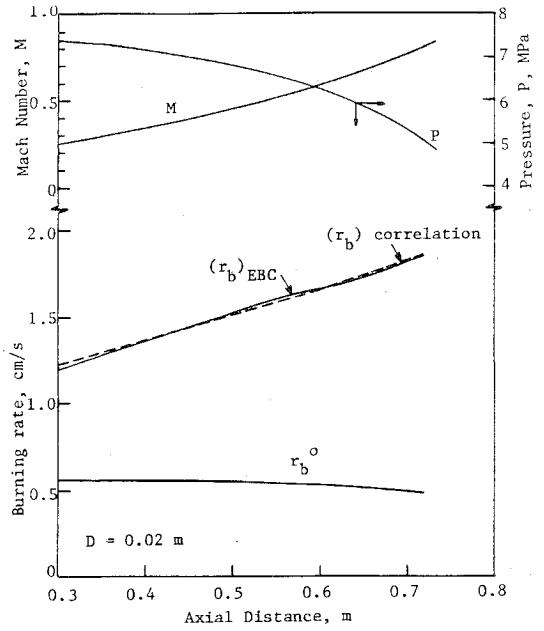

Fig. 7 Axial distribution of flow properties and burning rates in a constant-area cylindrical grain.

A comparison of predictions of this correlation [Eq. (11)] with data obtained for various values of M, P, R_h, $\partial P/\partial x$, D, and Tpi is presented in Fig. 6. The ranges of variation of these parameters are given in Table 2. The good agreement between data and overall correlation (represented by the 45-deg line) confirms that 1) the functional forms selected are adequate, and 2) the values of the constants in the correction factors are valid for the overall correlation. It is also evident that this correlation satisfies the limiting cases ($M \leq M_{th}$, $R_h = 0$, $\partial P/\partial x = 0$, $D = \infty$, and/or $Tpi = Tpi_r$) for all parameters.

Some examples which illustrate the application of this correlation are presented in the following section.

Examples

To illustrate the applications of Eq. (11), two examples involving different grain configurations were generated. These demonstrate the applicability of the correlation to grain design by showing the close agreement between results obtained from the correlation and from the EBC predictions. The computed flow property distributions are also useful in explaining the mechanism of erosive burning.

Example 1

The geometry considered was a constant area port with diameter of 0.02 m. Figure 7 shows the variation of M, P, r_b, and r_b^0 along the axial direction. The prediction of r_b using the correlation is also shown on the same figure by the dashed line which runs very close to the solid line of r_b predicted by EBC. The increase in M and decrease in P along the axial direction mainly is due to the mass addition. While r_b^0 decreases due to the decrease in P, r_b continues to increase axially due to the increase in M; this can be seen from Eq. (2). While the correction factor $f_{M,P}$ involves MP in the numerator, the effective exponent of P is lower than that of M, due to the presence of r_b^0 in the denominator.

The increase in r_b along the axis can also be explained in terms of the physical mechanism. Figure 8 shows the radial variation of mean velocity and turbulence kinetic energy at three axial locations. The increase in the centerline velocity leads to steeper velocity gradients near the propellant surface; this in turn increases the level of turbulence kinetic energy in this region. A direct consequence of this increase in turbulence kinetic energy is an increase in the degree of mixing of the

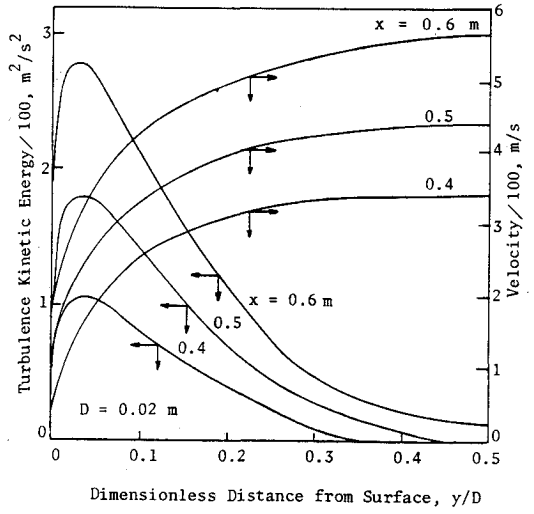

Fig. 8 Variation of velocity and turbulence kinetic energy profiles with axial distance.

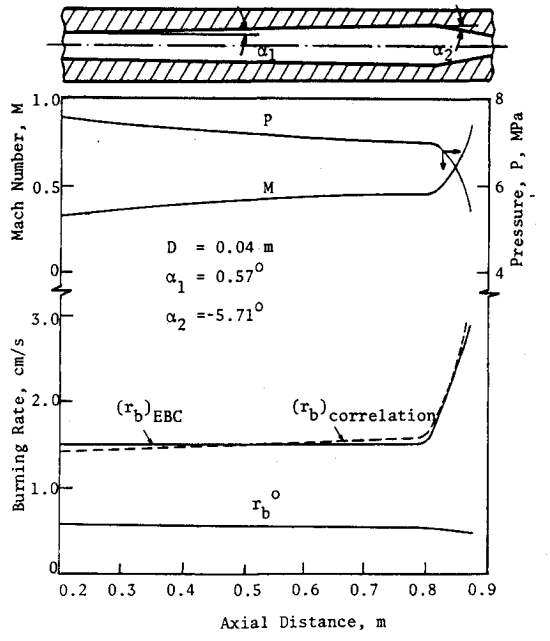

Fig. 9 Axial distribution of flow properties and burning rates in a variable-area cylindrical grain.

gaseous fuel-rich and oxidizer-rich mixtures, leading to higher heat release due to diffusive reaction close to the propellant surface. At the same time, the higher turbulence level enhances the turbulent transport properties. Both of these effects provide greater heat feedback from the flame zone to the propellant, thus increasing the burning rate.

Example 2

This example illustrates the effect of grain geometry on flow-property distributions and erosive-burning characteristics. It also demonstrates the ability of the correlation to predict a case involving surface roughness.

The grain configuration considered in this example is shown at the top of Fig. 9. The major portion of the grain is slightly divergent along its length, followed by a shorter convergent section. This particular geometry results in a large axial variation of flow conditions; the results are then used to test the accuracy of the correlation. As shown in Fig. 9, the burning rate is nearly uniform in the first section of the grain. There is some variation in M and P, but the effects of these

parameters on r_b compensate each other. In the convergent section, however, r_b rises sharply; this is intuitively obvious in the case of a protrusion in a rocket motor port. Several factors contribute to this augmentation in burning rate. Although P decreases, M increases and has a stronger influence on r_b, as explained in example 1. Other factors involved are stronger pressure gradient as well as smaller port diameter. Note that the solid and dashed lines still remain quite close, showing that the correlation is adequate even in regions where high gradients exist.

The preceding examples verify the fact that the correlation is, indeed, a useful and economical substitute for the numerical solution of the complete set of partial-differential equations. Also, since the correlation in Eq. (11) is based on data ranging through both subsonic and supersonic regions, it can be applied to high-performance or nozzleless motors. This correlation can be incorporated into ignition transient codes such as those described in Refs. 13 and 14, or into solid rocket performance prediction programs such as Solid Performance Program (SPP) described in Refs. 15 and 16. These programs can then be used to predict more accurately rocket motor performance, including time history of burning surface regression, pressure distribution, thrust level, and total burning time.

Conclusions

1) An erosive-burning rate correlation [Eq. (11)] has been developed, based on data obtained through parametric studies which used the erosive burning code (EBC). The validity of EBC was verified earlier by comparisons with a wide range of experimental data. The correlation, expressed in a simple algebraic form, includes the effect of Mach number, pressure, surface roughness, pressure gradient, port diameter, and initial propellant temperature. The asymptotic limits for all parameters are also matched.

2) The correlation predicts an increased burning rate for an increase in Mach number, pressure, surface roughness, favorable pressure gradient, curvature, and initial propellant temperature. Temperature sensitivity of the burning rate under erosive conditions is found to be lower than that of the strand burning rate. Therefore, as the initial propellant temperature increases, the burning rate augmentation factor decreases.

3) The applicability of this correlation to grain design is illustrated through two examples. Results showed close agreement between the burning rate predicted by the correlation and that obtained through numerical solution of the partial-differential equations; the physical mechanism of erosive burning is also delineated.

4) The procedure outlined in this paper is quite general and can be used to develop correlations for other types of propellants. Also, the functional form of Eq. (11) can serve as a guideline for developing erosive-burning correlations for various other composite solid propellants.

5) The overall erosive-burning correlation can be incorporated easily into an existing grain design procedure. Since it was developed for both subsonic and supersonic ranges of Mach number, it would be useful for nozzleless rocket motor design and interior ballistic calculations.

Acknowledgments

A part of this work was funded by a subcontract from the Atlantic Research Corporation which is the prime contractor for AFOSR (Contract No. F49620-78-C-0016) under the management of Dr. L.H. Caveny.

References

[1] Kuo, K.K. and Razdan, M.K., "Review of Erosive Burning of Solid Propellants," 12th JANNAF Combustion Meeting, CPIA Pub. 273, Vol. II, 1975, pp. 323-338.

[2] King, M.K., "Review of Erosive Burning Models," JANNAF Workshop on Erosive Burning/Velocity Coupling, Lancaster, Calif., March 1977.

[3] King, M.K., Kuo, K.K., Arora, R., and Beddini, R., "Experimental and Analytical Study of Erosive Burning of Solid Propellants," Final Report to U.S. Air Force Office of Scientific Research, ARC-TR-PL-5727-F, June 1981.

[4] Razdan, M.K. and Kuo, K.K., "Erosive Burning Study of Composite Solid Propellants by Turbulent Boundary-Layer Approach," *AIAA Journal,* Vol. 17, Nov. 1979, pp. 1225-1233.

[5] Razdan, M.K. and Kuo, K.K., "Turbulent Boundary-Layer Analysis and Experimental Investigation of Erosive Burning Problem of Composite Solid Propellants," Scientific Report to U.S. Air Force Office of Scientific Research, AFOSR-TR-79-1155, March 1979.

[6] Razdan, M.K. and Kuo, K.K., "Turbulent Flow Analysis of Erosive Burning of Cylindrical Composite Solid Propellants," *AIAA Journal,* Vol. 20, Jan. 1982, pp. 122-128.

[7] Patankar, S.V. and Spalding, D.B., *Heat and Mass Transfer in Boundary Layers,* Inter-text Books, London, 1970.

[8] Marklund, T. and Lake, A., "Experimental Investigation of Propellant Erosion," *American Rocket Society Journal,* Vol. 3, No. 2, 1960, pp. 173-178.

[9] Razdan, M.K. and Kuo, K.K., "Measurements and Model Validation for Composite Propellants Burning under Cross Flow of Gases," *AIAA Journal,* Vol. 18, June 1980, pp. 669-677.

[10] Arora, R., Kuo, K.K., and Razdan, M.K., "Turbulent Boundary Layer Flow Computations with Special Emphasis on the Near-Wall Region," *Proceedings of the AIAA 5th Computational Fluid Dynamics Conference,* June 1981, pp. 295-305.

[11] Spalding, D.B., "Mixing and Chemical Reaction in Steady Confined Turbulent Flames," *Thirteenth Symposium (International) on Combustion,* Combustion Institute, 1971, pp. 649-657.

[12] Yezzi, C.M., King, M.K., and Procinsky, I.M., "Improved Nozzleless Performance Program," 1981 JANNAF Propulsion Meeting, New Orleans, La., May 1981.

[13] Peretz, A., Kuo, K.K., Caveny, L.H., and Summerfield, M., "Starting Transient of Solid-Propellant Rocket Motors with High Internal Gas Velocities," *AIAA Journal,* Vol. 11, Dec. 1973, pp. 1719-1727.

[14] Caveny, L.H., Kuo, K.K., and Shackelford, B.W., "Thrust and Ignition Transients of the Space Shuttle Solid Rocket Motor," *Journal of Spacecraft and Rockets,* Vol. 17, Nov.-Dec. 1980, pp. 489-494.

[15] Coats, D.E. et al., "A Computer Program for the Prediction of Solid Propellant Rocket Motor Performance," Vols. I-III, AFRPL-TR-75-36, July 1975.

[16] George, D., Barger, M.E., and Smith, T.A., "Fators Affecting Delivered Performance in Solid Rocket Motors," *17th JANNAF Combustion Meeting,* CPIA Pub. 329, Vol. III, 1980, pp. 105-129.